Article ID: 1006-8775(2016) 02-0159-13

THE WARMING MECHANISM IN THE SOUTHERN ARABIAN SEA DURING THE DEVELOPMENT OF INDIAN OCEAN DIPOLE EVENTS

GUI Fa-yin (桂发银)[1], LI Chong-yin (李崇银)[1,2], TAN Yan-ke (谭言科)[1], LI Xin (黎 鑫)[1], XIA Lin-lin (夏淋淋)[1]

(1. College of Meteorology and Oceanography, PLA University of Science and Technology, Nanjing 211101 China;
2. LASG, Institute of Atmospheric Physics, Chinese Academy of Sciences, Beijing 100029 China)

Abstract: This study aims to explore the relative role of oceanic dynamics and surface heat fluxes in the warming of southern Arabian Sea and southwest Indian Ocean during the development of Indian Ocean Dipole (IOD) events by using National Center for Environmental Prediction/National Center for Atmospheric Research (NCEP/NCAR) daily reanalysis data and Global Ocean Data Assimilation System (GODAS) monthly mean ocean reanalysis data from 1982 to 2013, based on regression analysis, Empirical Orthogonal Function (EOF) analysis and combined with a $2^1/_2$ layer dynamic upper-ocean model. The results show that during the initial stage of IOD events, warm downwelling Rossby waves excited by an anomalous anticyclone over the west Indian Peninsula, southwest Indian Ocean and southeast Indian Ocean lead to the warming of the mixed layer by reducing entrainment cooling. An anomalous anticyclone over the west Indian Peninsula weakens the wind over the Arabian Sea and Somali coast, which helps decrease the sea surface heat loss and shallow the surface mixed layer, and also contributes to the sea surface temperature (SST) warming in the southern Arabian Sea by inhibiting entrainment. The weakened winds increase the SST along the Somali coast by inhibiting upwelling and zonal advection. The wind and net sea surface heat flux anomalies are not significant over the southwest Indian Ocean. During the antecedent stage of IOD events, the warming of the southern Arabian Sea is closely connected with the reduction of entrainment cooling caused by the Rossby waves and the weakened wind. With the appearance of an equatorial easterly wind anomaly, the warming of the southwest Indian Ocean is not only driven by weaker entrainment cooling caused by the Rossby waves, but also by the meridional heat transport carried by Ekman flow. The anomalous sea surface heat flux plays a key role to damp the warming of the west pole of the IOD.

Key words: Arabian Sea; summer monsoon; Indian Ocean Dipole; $2^1/_2$ layer dynamic upper-ocean model

CLC number: P732 **Document code:** A

doi: 10.16555/j.1006-8775.2016.02.006

1 INTRODUCTION

The Indian Ocean Dipole (IOD) is an east-west oscillation mode of sea surface temperature anomaly (SSTA) in the equatorial Indian Ocean. Although early studies suggested that the IOD was a coupled ocean-atmosphere phenomenon independent of ENSO occurring in the tropical Indian Ocean (Saji et al.[1]; Webster et al.[2]; Yamagata et al.[3]), later research showed that it has a strong relationship with ENSO (Li and Mu.[4]; Xie et al.[5]; Li et al.[6]; Wang et al.[7]; Yuan et al.[8]). The IOD has a significant impact on the weather and climate in its vicinity through its influence on lower atmosphere circulation anomalies, and is also responsible for anomalous activity of the Asian-Australian monsoon system (Saji et al.[1]; Li and Mu[4]; Guan and Yamagata[9]; Yang and Ding[10]; Yu and Guan[11]). During positive IOD events, a negative SSTA occurs along the tropical southeast Indian Ocean coast of Sumatra, while a positive anomaly occurs in the tropical west Indian Ocean, and easterly wind anomalies occur in the east-central equatorial Indian Ocean. Southeasterly wind anomalies off the coast of Sumatra strengthen the climatological southeast wind, leading to an increase in the sea surface heat loss and a shallowing thermocline layer; they also contribute to SST cooling, which stimulates an anomalous anticyclone over the southeast Indian Ocean (Gill[12]) that further strengthens the southeasterly wind anomalies and SST cooling off the coast of Sumatra. The anomalous anticyclone leads to SST warming in the southwest Indian Ocean by stimulating westward propagating warm Rossby waves south of the equator. The seasonal dependence of such a feedback mechanism means that the IOD is phase-locked in September (Li et al.[6]; Tan et al.[13]). Cold eastward propagating Kelvin waves along the equator and warm westward propagat-

Received 2015-11-20; **Revised** 2016-02-16; **Accepted** 2016-04-15

Foundation item: National Natural Science Foundation (41490642, 41205073); National Basic Theoretical Research Project (2015CB453200)

Biography: GUI Fa-yin, Ph.D. candidate, associate researcher, primarily undertaking research on monsoon and Indian Ocean Dipole.

Corresponding author: LI Chong-yin, e-mail: lcy@lasg.iap.ac.cn

ing Rossby waves off the equator excited by the east wind anomalies in the east-central equatorial Indian Ocean can lead to cooling of the southeast Indian Ocean and warming of the southwest Indian Ocean in the early stage of development of the positive IOD event. (Webster et al.[2]; Tan et al.[13]; Vinayachandran et al.[14]; Murtugudde et al.[15]; Rao et al.[16]; Yuan and Liu[17]).

How does the northwest Indian Ocean get warm during the development of an IOD event? Some research suggests that El Niño can excite an anomalous anticyclone over the southeast Indian Ocean and hence a westward propagating warm Rossby wave, thereby creating anomalously warm SST in the southwest Indian Ocean (Xie et al.[5]; Li et al.[6]; Wang et al.[7]). This warm anomaly may lead to a cross-equatorial gradient in the western Indian Ocean and trigger an asymmetric wind pattern with northeasterly anomalies north of the equator and northwesterly anomalies south of the equator (Wu et al.[18]; Du et al.[19]; Guo et al.[20]). When the southwesterly monsoon occurs in boreal summer, the northeasterly anomalies in the northwestern Indian Ocean counteract the background winds, favoring local SST warming over the south of the Arabian Sea by reducing evaporation in June-July. Based on the atmospheric bridge theory, Yuan et al.[8] believe that El Niño can lead to the warming in the northwestern Indian ocean by relatively less latent heat loss from the ocean due to reduced wind speed and the deepened thermocline along the east coast of Africa through the suppressed upwelling of the cold water.

Prasad and McClean [21] argued that the mechanism of warming the Arabian Sea area is mainly an oceanic internal process rather than a direct response to external forcing from the eastern Indian Ocean. In a normal year, the existence of a unique open ocean upwelling feature, the Arabian Sea Dome (ASD), raises the thermocline in the south Arabian Sea, which is a result of the positive wind stress curl in the winter monsoon. During an IOD year, the monsoon wind system in the Arabian Sea collapses and the cold tongue fails to develop. The thermocline remains deep, which in turn enhances the heat content of the upper ocean, leading to warmer SST. Guo et al.[22] suggested that warm SST in the southeastern Arabian Sea (SEAS) and cold SST to the southeast of the SEAS result in the intensification of the southeasterly anomaly in the tropical Indian Ocean, which transports more moisture to the SEAS, thereby enhancing precipitation in this region. The ocean-atmosphere interaction process, involving the wind, precipitation, the barrier layer and SST, is important for the anomalous warming in the SEAS during the development of positive IOD events. In addition, the weakening of the summer monsoon in the northern Indian Ocean can lead to a positive SST anomaly off western India (Murtugudde et al.[15]; Li et al.[6]; Yuan et al.[8]).

In summary, there is now a greater understanding of the physical mechanisms responsible for the cooling of the southeast Indian Ocean and warming of the southwest Indian Ocean, while there remain some conflicting views about the warming process of the northwest Indian Ocean during the development of IOD events. How does the monsoon anomaly over the Arabian Sea affect the warming in the northwest Indian Ocean during the IOD event? Is the same mechanism responsible for warming in the northwest and southwest Indian Ocean? These questions require further study.

The remainder of this paper is organized as follows. Section 2 briefly describes the data sources and methods. Sections 3 and 4 mainly discuss the different warming mechanisms in the south Arabian Sea and southwest Indian Ocean with reanalysis data and model simulations. Finally, section 5 presents the conclusions and discussion.

2 DATA, METHODS AND MODEL

2.1 *Data*

The primary data used here are the daily 10-m wind, 2-m air temperature, sea surface momentum flux, 2-m specific humidity, surface latent heat net flux, surface sensible heat net flux, and radiation flux (1980–2013) extracted from the NCEP_Reanalysis 2 data provided by the NOAA/OAR/ESRL PSD, Boulder, Colorado, USA (http://www.esrl.noaa.gov/psd/), on a global T62 Gaussian grid (192×94). Monthly mixed layer depth, isothermal layer depth, ocean current, ocean temperature and sea surface height data (1980–2013) are taken from GODAS data provided by the NOAA/OAR/ESRL PSD with a spatial resolution of 1°×1°(enhanced to 1/3°×1/3° at latitudes within 10° of the equator). We also use the daily high-resolution blended analyses of SST data (1982–2013) with 0.25°×0.25° resolution from the NOAA to construct the IOD/IOZDM index (following the definition of Saji et al.[1]). Since the IOD events are interannual variability modes and may have a close relationship with an intraseasonal signal (Wilson et al.[23] Rao et al.[24]; Du et al.[25]), a 5-720 pentad band-passing filter is applied to extract the signal from the intraseasonal time scale to the interannual time scale during the following data analysis.

2.2 *Methods and model*

The primary methods used in this study are regression analysis, Empirical Orthogonal Function (EOF) analysis, and numerical simulations using a $2^1/_2$ layer dynamic upper-ocean model developed by McCreary et al.[26, 27]. The model has two active layers overlying a deep motionless layer of infinite depth. The first layer can split into a mixed layer with the entrainment and detrainment processes generated by wind stirring and

cooling at the surface (Kraus and Turner[28]) and a non-turbulent "fossil layer" isolated from the surface forcing but can be engulfed into the mixed layer during strong entrainment or in upwelling regions. The model's second layer, in turn, is driven by the mass and heat fluxes derived from the first layer. Because there is considerable entrainment into the first layer, there must be detrainment through the base of the first layer for mass continuity. This process simulates the subduction of surface layer water into the thermocline. The southern boundary and the Indonesian Throughflow (ITF) of the model do not correspond to any real boundary in the Indian Ocean, and zero-gradient open-boundary conditions are applied there, while closed-boundary conditions are used at other boundaries. In this paper we simulate the area 30°S–25°N, 35°–115°E with an improved model resolution of 0.2°×0.2° driven by surface air temperature, surface winds at 10 m, surface momentum flux, specific humidity, and net solar radiation which provided by the NOAA/OAR/ESRL on a global T62 Gaussian grid for the period 1980–2013. The model-simulated mixed layer temperature is used for the sensible and latent heat flux computations. The model is integrated forward in time with a time step of 120 seconds and spun up from a state of rest beginning on January 1, 1980 and keeping running about 5 years, by which time the model reached a stable condition before the formal simulation running from January 1, 1980 to December 31, 2013. The data used to diagnose the evolution of IOD events were selected from the model output for the period 1982–2013 except for the first two years.

3 DATA ANALYSIS

3.1 *Relationship between surface wind anomalies, SSTA, and the IOD*

To reveal the effect of the sea surface wind field on SST, the lag regressions of the SSTA and sea surface wind stress anomalies are calculated (Fig.1) with respect to the IOD index (Saji et al.[1]). The panels in Fig.1 refer to the number of pentads before (negative) or after (positive) an IOD maximum. From –24 to –18 pentads, there is a weak cold SSTA off the western coast of the Indian Peninsula, followed by a weak warm SSTA in the southeast and southwest Arabian Sea and north of Madagascar. A southwesterly wind anomaly appears over the central-eastern Arabian Sea and a weak easterly wind anomaly appears over the equatorial western Indian Ocean. From –15 to –9 pentads the SST increase expands to cover the whole western Indian Ocean west of the Indian Peninsula and north of Madagascar, including the southeast and southwest Arabian Sea. Southwesterly and southeasterly wind anomalies appear in the north and southeast Arabian Sea, respectively, and a significant easterly wind anomaly appears in the equatorial Indian Ocean. Finally, in the 6 pentads preceding the IOD event, the southwesterly wind anomaly gradually disappears over the northern Arabian Sea, a strong easterly wind anomaly appears over the South Arabian Sea, and a significant northeasterly wind anomaly occurs along the coast of Somalia as the IOD reaches a maximum.

Figure 2 shows the IOD index with the surface 10-m wind anomaly and surface wind stress curl anomaly lag regression. Between –24 and –18 pentads, a negative wind stress curl anomaly first appears over the Indian Peninsula while a positive anomaly appears over the southwest and southeast Indian Ocean. A negative 10-m wind anomaly appears over the southeast Arabian Sea and the coast of Somalia. Then, from –15 to –9 pentads there is a negative wind stress curl anomaly west of the Indian Peninsula, and a positive anomaly in the southwestern and southeastern Indian Ocean. The area of positive wind stress curl gradually expands and its intensity increases. Two negative 10-m wind anomaly centers appear over the southeast Arabian Sea and Somali coast. Finally, in the 6 pentads prior to the maximum IOD, the wind stress curl anomaly is still negative in the western Indian Peninsula, and positive in the southwest and southeastern Indian Ocean. There is still a strong negative wind speed anomaly in the south Arabian Sea, but no significant effect on the wind in the southwest Indian Ocean during this period.

According to the above analysis, there are obvious differences in the distribution of the wind field over the southern Arabian Sea and the southwest Indian Ocean during the development of IOD events. Warm downwelling Rossby waves (Fig.3: c1, c2, c3) excited by an anomalous anticyclone over the western Indian Peninsula and the southwest and southeast Indian Ocean deepen the thermocline and increase the thermocline heat content, which then leads to mixed layer warming by entrainment and advection. The anomalous anticyclone over the western Indian Peninsula based on the climatic summer westerly winds produces two 10-m wind negative anomaly centers over the Arabian Sea and Somali coast, which lead to a further decrease in upward heat flux from the sea surface and shallowing of the surface mixed layer (Fig.3: b1, b2, b3). The anticyclone also contributes to increasing SST by affecting ocean dynamical processes, such as mixed layer advection and entrainment. Warming over the southwest Indian Ocean is closely connected with the Rossby waves excited by the anomalous anticyclone over the southeast and southwest Indian Ocean. Wind anomalies over the southwest Indian Ocean are not significant.

3.2 *Effect of sea surface heat flux on SSTA*

Figure 4 shows the IOD index with the sea surface

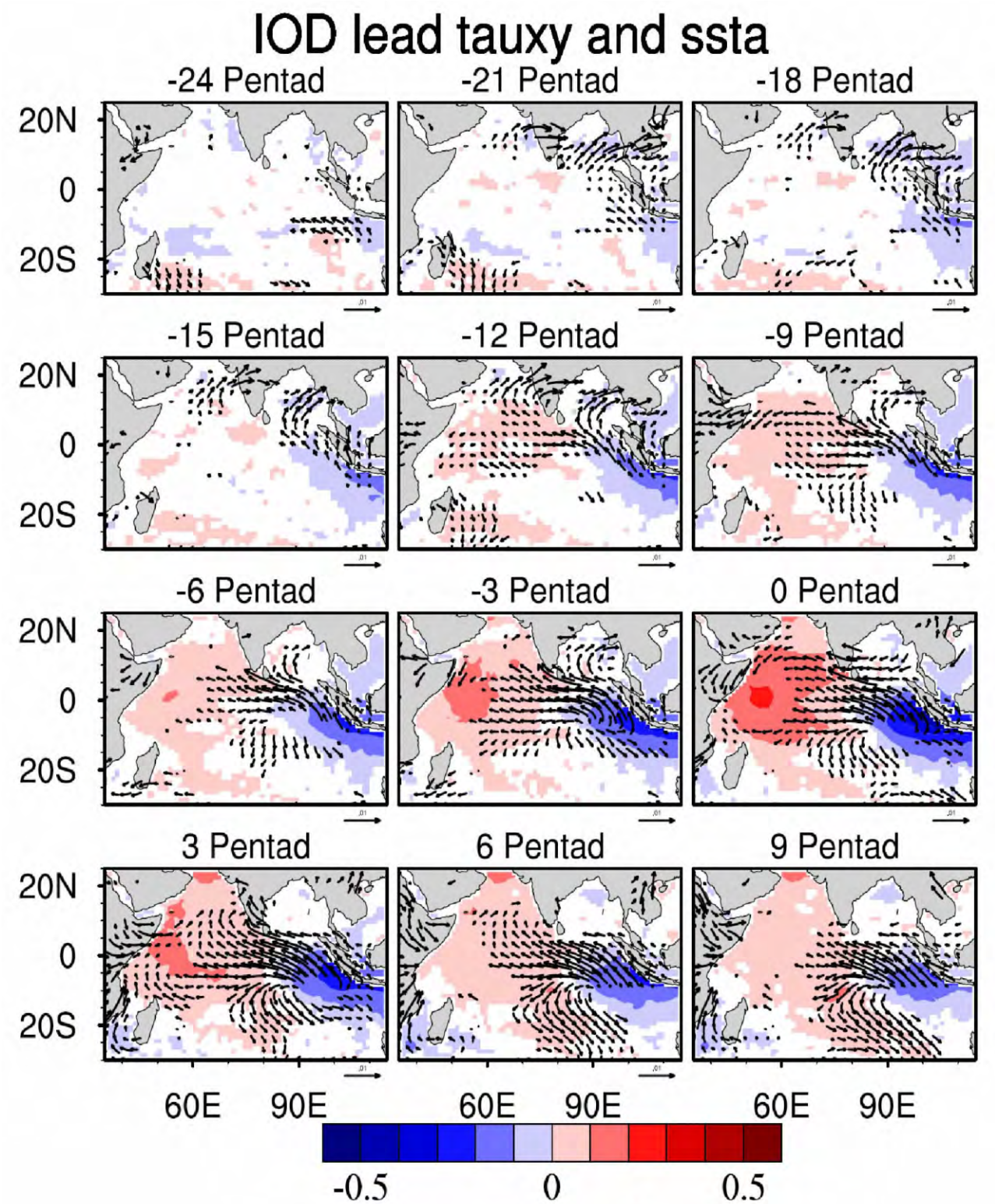

Figure 1. Lag regressions of surface momentum flux anomalies (vectors; N m^{-2}) and SSTA (shaded; ℃). Values above the 95% significance level are plotted. The IOD index is used for standardization. Positive lag indicates the IOD index time series is leading, and vice versa. The same filtering and standardization process is applied in the following figures.

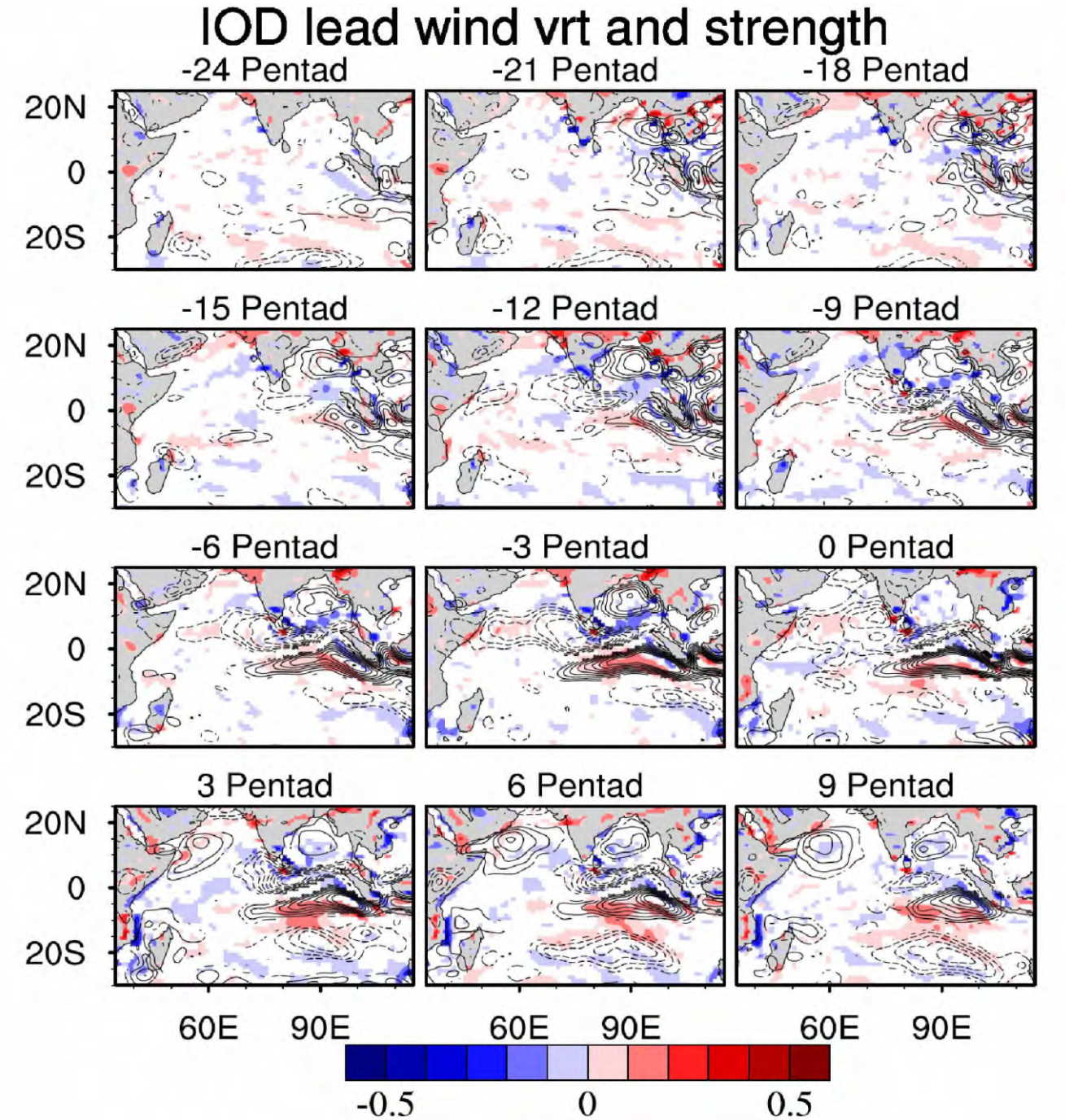

Figure 2. Lag regressions of 10-m wind speed anomalies (contour interval is 0.3 m s^{-1}; dashed line indicates negative values) and wind stress curl anomalies (shaded; units: 10^{-7} N m^{-3}).

net heat flux anomaly lag regression. Initially, positive anomalies of sea surface heat flux (Fig.4: −24 to −12 pentads) and negative anomalies of mixed layer depth (Fig.3: b1, b2, b3) further enhance the contribution of the net heat flux to the mixed layer temperature over the southern Arabian Sea. There is no obvious heat flux anomaly in the southwest Indian Ocean (10°S–0°), but the mixed layer deepens (Fig.3: b1, b2, b3), which weakens the contribution of the sea surface heat flux to the mixed layer temperature anomaly. From −9 pentads to the IOD maximum, the positive anomalies of surface heat flux in the northwest Indian Ocean is not significant, while a negative net heat flux anomaly appears in the southwest Indian Ocean, damping the warming of

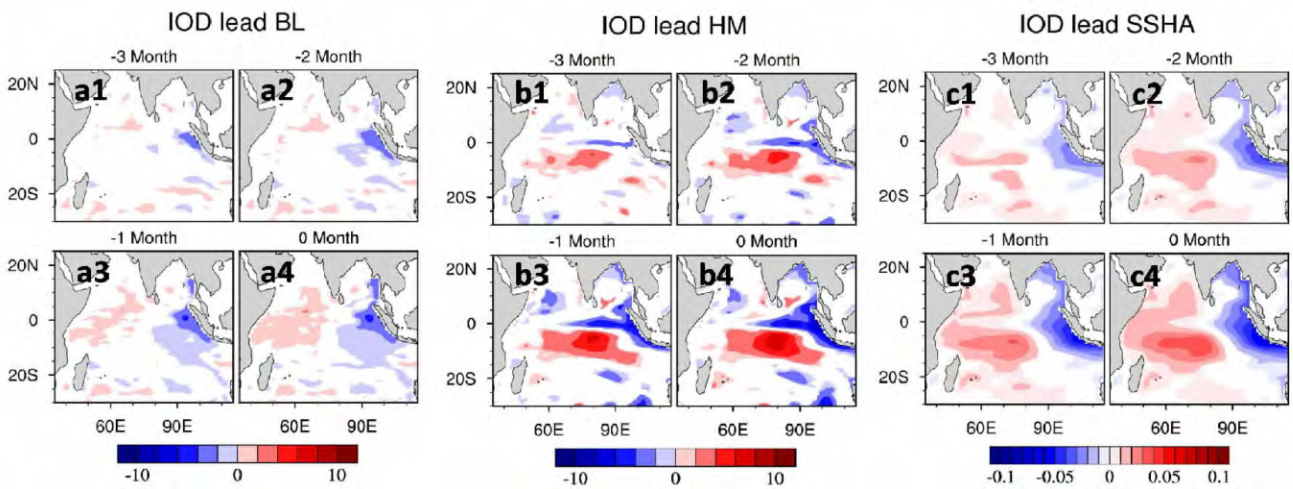

Figure 3. Lag regressions of (a1–a4) barrier layer thickness anomaly, (b1–b4) mixed layer depth anomaly, and (c1–c4) sea surface height anomaly. All quantities are in meters.

the southwest Indian Ocean. The contribution of sea surface heat flux in the south Arabian Sea is significantly greater than in the southwest Indian Ocean during the initial stage of IOD events (about −24 to −12 pentads), but closer to the IOD event (from about −9 pentads) the major contribution of the sea surface heat flux to the west pole of the IOD is the cooling.

4 NUMERICAL SIMULATIONS OF THE $2^1/_2$ LAYER DYNAMIC UPPER-OCEAN MODEL

4.1 *Validation of the simulations*

The above analysis suggests that the south Arabian Sea and southwest Indian Ocean may have different warming mechanisms. To further diagnose the relative roles of dynamic and thermodynamic processes in the development of the IOD over the southern Arabian Sea and southwest Indian Ocean, a $2^1/_2$ layer dynamic upper-ocean model was used to simulate the characteristics of mixed layer temperature in the tropical Indian Ocean. After a 5-year spin-up the model became stable and the simulation was begun. Data for the first two years are discarded, and the simulation data for 1982–2013 are diagnosed.

Figure 5 shows the climatology of the mixed layer flow field which is calculated from the average of the flow field over the mixed layer depth and provided by the $2^1/_2$ layer dynamic upper-ocean model and the corresponding GODAS data. The model can simulate the main circulation characteristics of the Indian Ocean, but a further comparison shows that the Somali Current in summer and the Wyrtki Jet in autumn are too strong and north equatorial flow is too weak in winter.

Figure 6 shows the EOF analysis of the mixed layer temperature anomaly of the model and GODAS which is calculated from the average of the temperature anomaly over the mixed layer depth. The results show that the spatial distribution of the EOF first mode closely resembles that of the Indian ocean Basin Mode (IOBM), while the EOF second mode closely resembles the IOD mode; however, the simulated peak of the dipole mode is slightly to the east, and it is too strong in the southwest of the Indian Peninsula. The coefficients of the EOF second mode for the model and GODAS both have significant interannual variation, and their correlation coefficient reaches 0.89 (significant at the 99.9% level). Overall, this model can simulate well the upper surface temperature variability in the Indian Ocean.

4.2 *Model analysis*

We now consider in more detail the physical processes of the mixed layer in the development of the IOD. The temperature Tm of the mixed layer is determined in the 2.5 layer model from

$$\frac{\partial T_m}{\partial t}=-u_1\cdot\partial T_m/\partial x-v_1\cdot\partial T_m/\partial y+\kappa_t\nabla^2 T_m+Q/h_m+L \quad (1)$$

where $L=-\delta[W_e\theta(W_e)(T_m-T_e)/h_m]-\phi[W_k\theta(W_k)(T_m-T_f)/h_m]$, u_1 is zonal velocity in the upper layer, v_1 is meridional velocity in the upper layer, Q is the net downward heat flux at the sea surface, h_m is mixed layer thickness, T_e is the temperature of water entrained into the upper layer, T_f is the temperature in the fossil layer, and δ, θ, and ϕ are Heaviside step functions (McCreary et al.[26, 27]).

Using perturbation analysis, Eq.(1) can be written as:

$$\frac{\partial T'_m}{\partial t}=A_1'+A_2'+A_3'+A_4'+A_5' \quad (2)$$

where $T_m=\overline{T_m}+T'_m$; $-u_1\cdot\partial T_m/\partial x=-\overline{u_1}\cdot\partial\overline{T_m}/\partial x+A_1'$; $-v_1\cdot\partial T_m/\partial y=-\overline{v_1}\cdot\partial\overline{T_m}/\partial y+A_2'$; $\kappa_t\nabla^2 T_m=\kappa_t\nabla^2\overline{T_m}+A_3'$; $Q/h_m=\overline{Q}/\overline{h_m}+A_4'$;

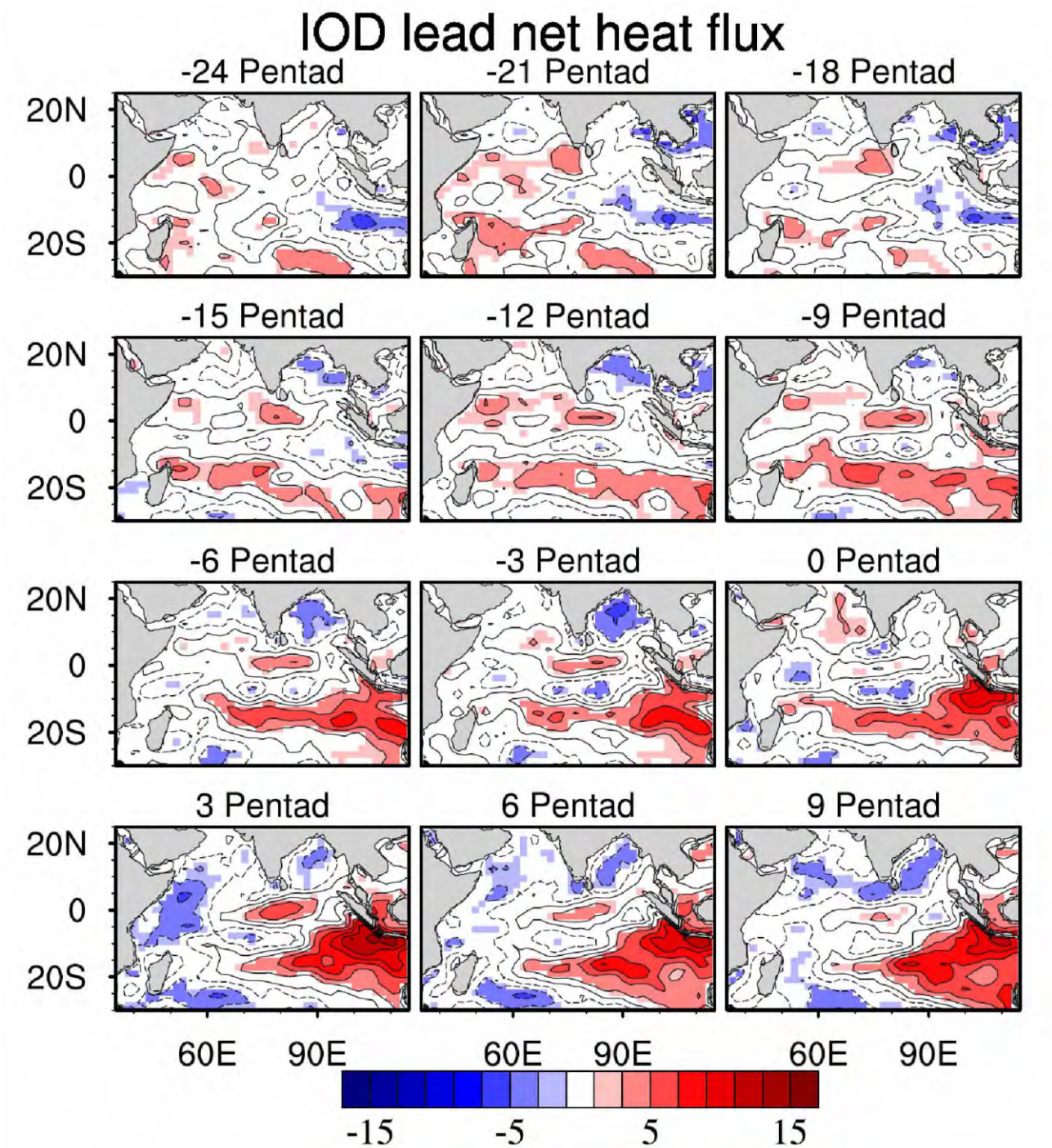

Figure 4. Lag regressions of sea surface heat flux anomaly. Positive regression coefficients for the net surface heat flux denote heat transferred from atmosphere to ocean. Contour interval is 2.0 W m^{-2} $℃^{-1}$ (units: W m^{-2} $℃^{-1}$).

$L=\bar{L}+A_5'$

The left hand side of Eq.(2) is the total temperature tendency, and the right hand side consists of terms that affect the mixed layer temperature. Of the five terms on the right hand side of Eq.(2), the first is the zonal advective heat transport anomaly (A_1'), the second is the meridional advective heat transport anomaly (A_2'), the third is the nonlinear diffusion anomaly(A_3'), the fourth is the net surface heat flux anomaly(A_4'), and the fifth term is the anomalous vertical entrainment mixing (A_5').

4.2.1 SPATIO-TEMPORAL VARIABILITY OF THE MIXED LAYER TEMPERATURE TENDENCY EQUATION

Figure 7 shows the lag regression of the different anomaly terms ($\partial T_m/\partial t$, A_1', A_2', A_3', A_4', A_5') in the mixed

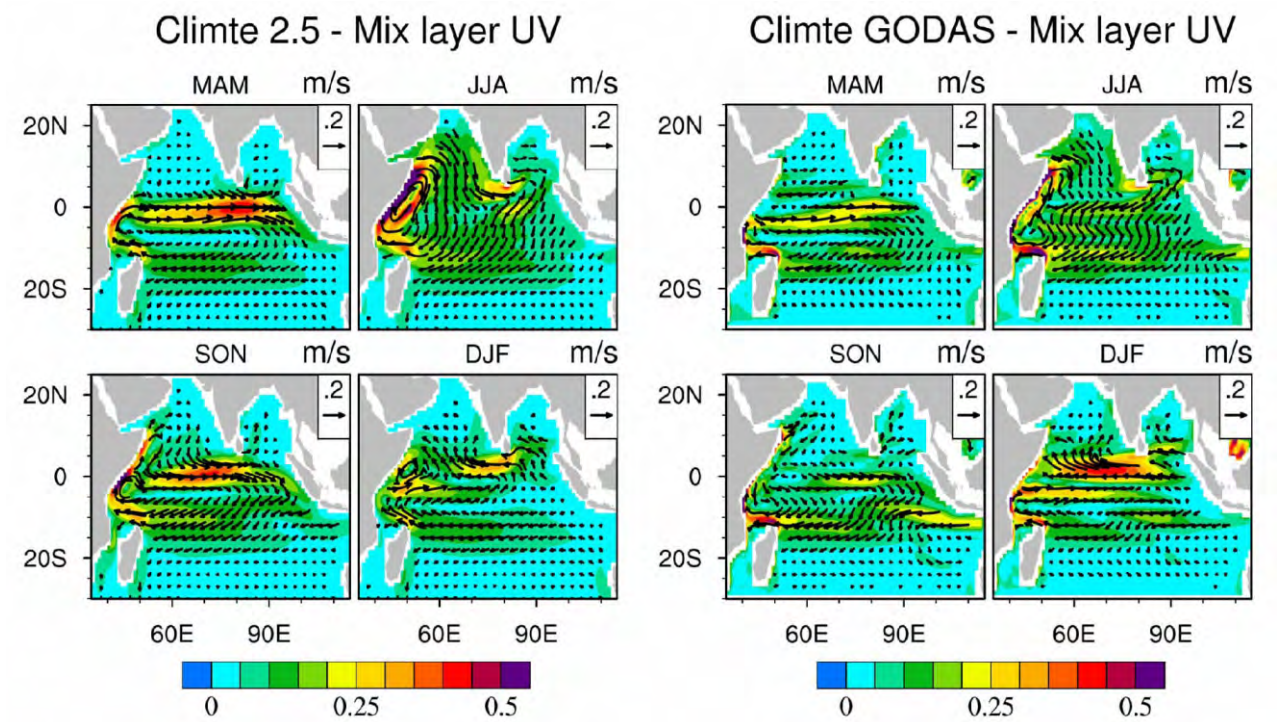

Figure 5. Seasonal distributions of mixed layer flow field (vectors; m s^{-1}) and strength of flow velocity (shaded ; m s^{-1}) from the $2^{1}/_{2}$ layer dynamic upper-ocean model (left) and GODAS data (right). All data are interpolated into 1°×1°.

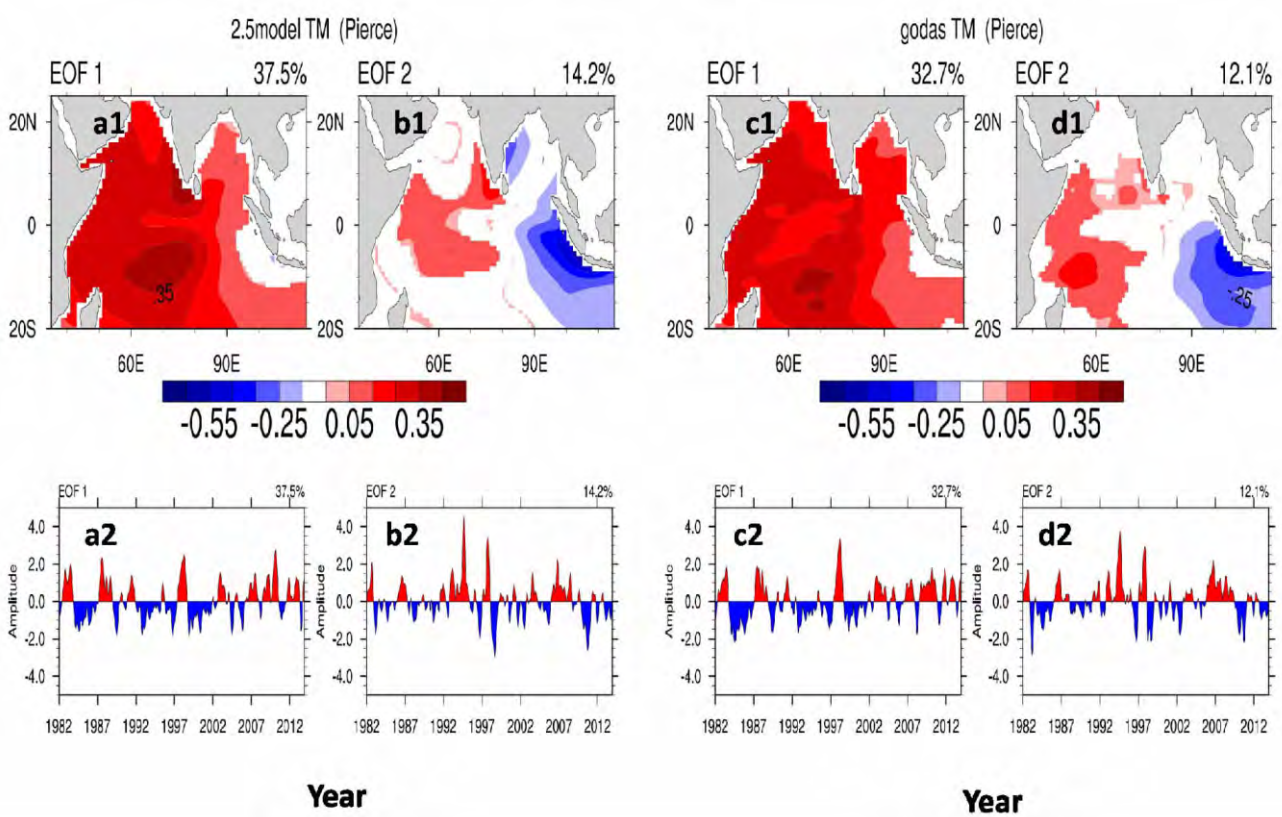

Figure 6. Normalized time varying coefficients (NTC) and spatial distributions (Regressions of the mixed layer temperature anomaly with the NTC, Values above the 95% significance level are plotted) of the first 2 modes obtained by EOF analysis of the mixed layer temperature anomalies (units: ℃) from the $2^{1}/_{2}$ layer dynamic upper-ocean model data (left) and GODAS data (right). Spatial distributions: a1, b1, c1, d1. Time coefficients: a2, b2, c2, d2. All data are interpolated into 1°×1°.

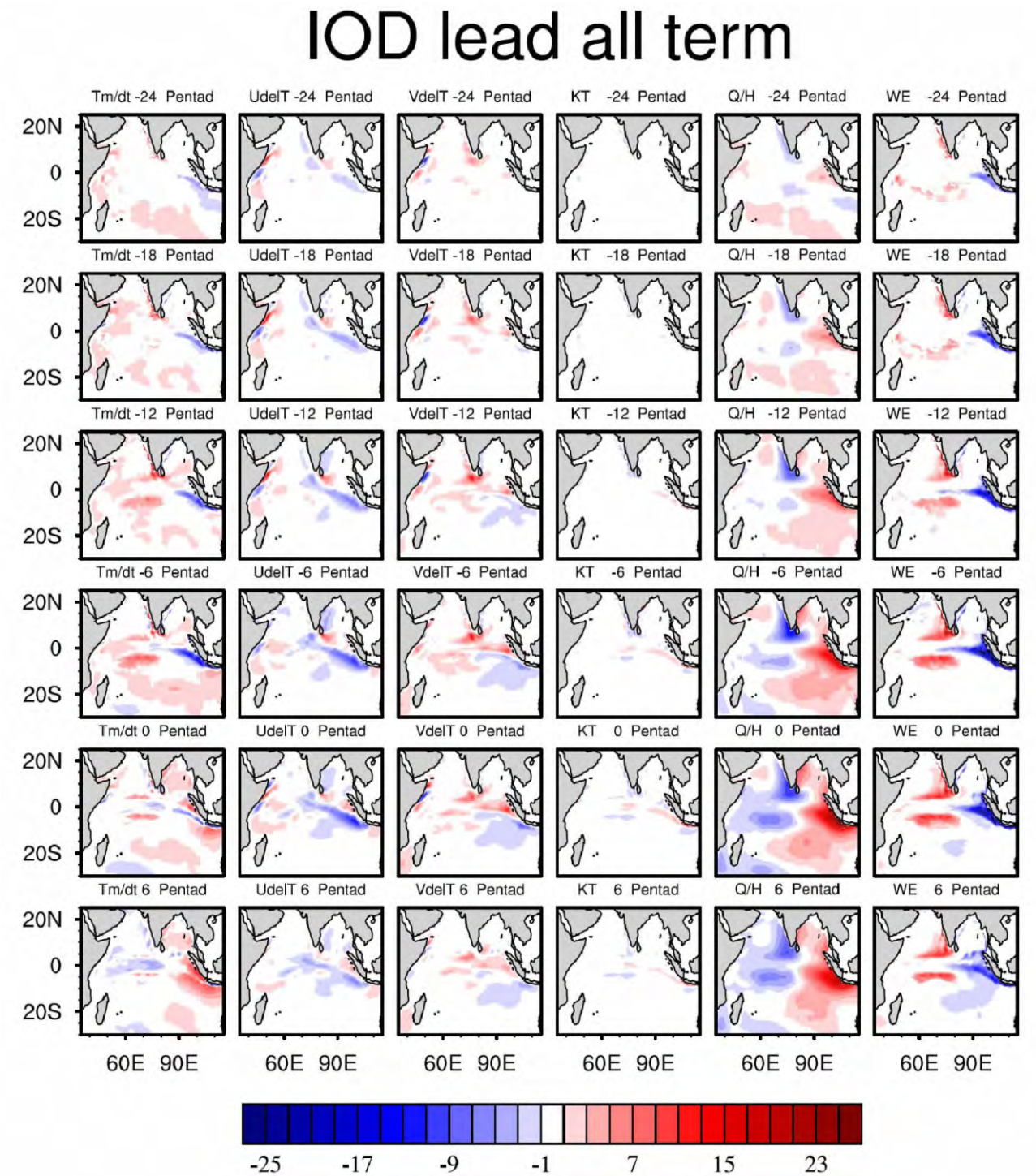

Figure 7. Lag regressions of the anomaly terms in Eq.(2) (units: 10^{-8} ℃ s^{-1}). The MIOD index is used for standardization. First column is the total temperature tendency $\partial T'_m/\partial t$; second column is the zonal advective heat transport anomaly A'_1; third column is the meridional advective heat transport anomaly A'_2; fourth column is the nonlinear diffusion anomaly A'_3; fifth column is the net surface heat flux anomaly A'_4; and sixth column is the anomalous vertical entrainment mixing A'_5.

layer temperature tendency Eq. (2) with respect to the model IOD (MIOD) index. The temperature tendency term anomaly ($\partial T'_m/\partial t$, Fig.7: first column) shows warming of the Arabian Sea and off the coast of Somalia appearing first (−24 to −18 pentads), and then the southwest Indian Ocean begins to warm rapidly (−12 pentads to the IOD maximum). The zonal advective heat transport anomaly (A'_1, Fig.7: second column) shows a strong positive anomaly over the coast of Somalia but a weak anomaly in the southwest Indian

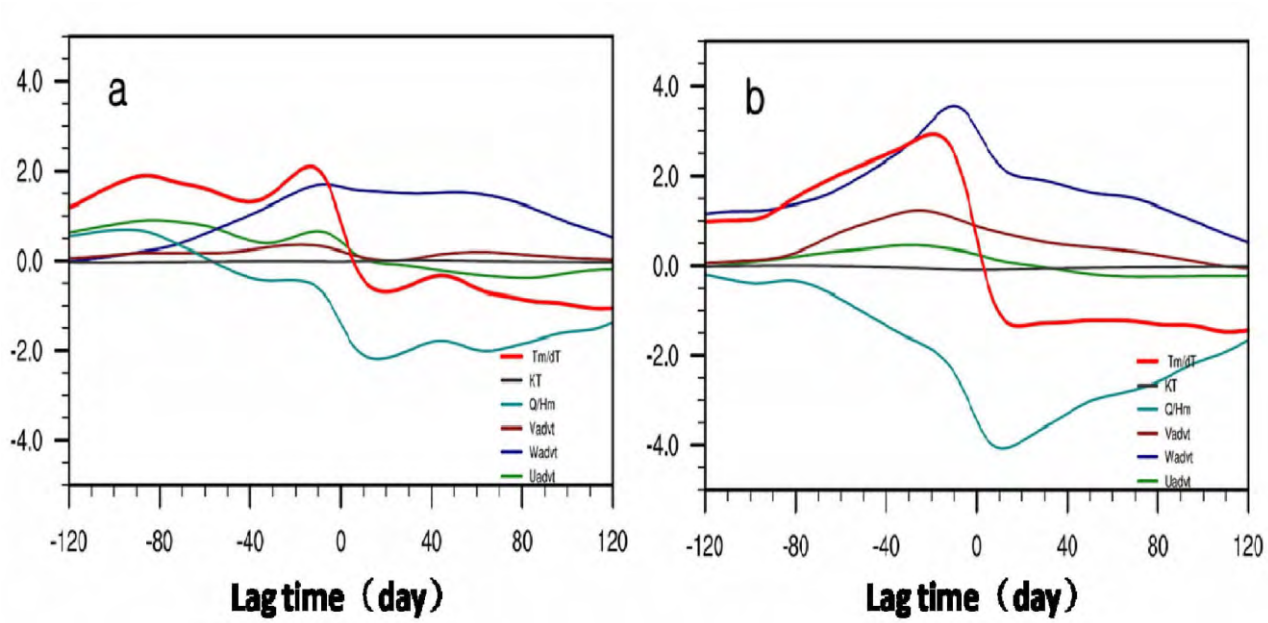

Figure 8. Lag regressions of the mixed layer temperature tendency and individual anomaly terms (units: 10^{-8} ℃ s^{-1}) with respect to the MIOD index for (a) the southern Arabian Sea and (b) the southwest Indian Ocean (Positive lag indicates the MIOD index time series is leading, and vice versa). Red lines denote the temperature tendency $\partial T'_m/\partial t$, light green lines denote the zonal advection heat transport anomaly A'_1, brown lines denote the meridional advection heat transport anomaly A'_2, dark green lines denote the sea surface heat flux anomaly A'_4, and blue lines denote the vertical entrainment anomaly A'_5.

Ocean. There is a positive meridional advective heat transport anomaly (A'_2, Fig.7: third column) in the southeast Arabian Sea and southwest Indian Ocean. The impact of the nonlinear diffusion anomaly (A'_3, Fig.7: fourth column) is weak. The net surface heat flux anomaly (A'_4, Fig.7: fifth column) shows that the central Arabian Sea receives a net heat input while the southeast Arabian Sea and southwest Indian Ocean lose heat (fifth column: −24 to −12 pentads). At the IOD west pole, there are strongly negative surface net heat flux anomalies on both sides of the equator (fifth column: from −6 pentads to the IOD event). A positive anomaly of vertical entrainment mixing (A'_5, Fig.7: sixth column; −24 to −12 pentads) appears in the southeast Arabian Sea and southwest Indian Ocean. This positive anomaly of vertical entrainment mixing in the southeast Arabian Sea gradually extends southward and westward to the south Arabian Sea while strengthening, leading to warming in the West Indian Ocean. In contrast to the negative net heat flux anomalies either side of the equator in the Indian Ocean west pole, the vertical entrainment mixing anomalies are strongly positive (sixth column: −6 to 0 pentads).

4.2.2 RELATIVE ROLES OF DIFFERENT TERMS IN EQ.(2) IN TERMS OF WEST POLE WARMING

Figure 8 (a and b) shows the time variation of the temperature tendency anomaly ($\partial T'_m/\partial t$) and other anomaly terms (A'_1, A'_2, A'_3, A'_4, A'_5) from Eq.(2) over the south Arabian Sea (0°−10°N, 50°−70°E) and southwest Indian Ocean (10°S−0°, 50°−70°E), respectively, during the development of an IOD event (the MIOD index is used).

In the south Arabian Sea, from 120 to 60 days before the IOD event there is a positive anomaly of sea surface heat flux (−24 to −12 pentads; Figs.4 and 7: fifth column) and an anomalously shallow mixed layer (Fig.3: b1, b2), leading to the sea surface heat flux playing an important role in warming at this stage (Fig. 8a). A negative wind anomaly (Fig.2: −24 to −12 pentads) along the coast of Somalia suppresses upwelling, resulting in a zonal advective heat transport anomaly (Fig.7, second column: −24 to −12 pentads) that also leads to warming over the south Arabian Sea. Then, from 60 to 10 days before the IOD event, an anomalous anticyclone over the west Indian Peninsula excites a warm downwelling Rossby wave (Fig.3: c2, c3) and weakens the wind velocity over the south Arabian Sea and Somali coast (Fig.2: −9 to −3 pentads). This weakened wind leads to shallowing of the surface mixed layer (Fig.3: b2, b3) and deepening of the barrier layer (Fig.3: a2, a3), which then contributes to increasing SST in the south Arabian Sea and off the Somali coast by inhibiting entrainment and zonal advective heat transport, respectively. The net heat flux anomaly changes from positive to negative, playing the role of a damping cooling in the southern Arabian Sea (Fig.8a). Then, in the

10 days before the IOD event, entrainment (Fig.7, sixth column: 0 pentads) still makes a relatively large contribution to mixed layer temperature over the southern Arabian sea, while the contribution of the zonal and meridional advective heat transport anomalies (Fig.7, first and second columns, 0 pentad) off the Somali coast gradually weakens and the damping cooling effect of the sea surface net heat flux anomaly over the southern Arabian Sea is suddenly enhanced (Fig.7, fifth column: 0 pentad). In the extinction stage (during the 80 days after the event), although the contribution of entrainment to the mixed layer temperature anomalies is still significant, the negative sea surface net heat flux anomaly is dominant and enhanced wind speed (Fig.2: +3 pentads) along the coast of Somalia means that the negative zonal advective anomaly appears to lead to cooling of the south Arabian Sea.

In the southwest Indian Ocean (Fig.8b) between 120 and 80 days before the IOD event, a warm downwelling Rossby wave (Fig.3: c1) excited by an anomalous anticyclone (Fig.2: −24 to −12 pentads) over the southwest Indian Ocean leads to deepening of the thermocline (Fig.3: b1, b2), which weakens the influence of the sea surface net heat flux and strengthens mixed layer temperature warming by entrainment (Fig.8b: −120 to 80 days). In the next 80 days (−80 to 0) the warm downwelling Rossby wave (Fig.3: c2, c3) between the southwest and southeast Indian Ocean, excited by the corresponding atmospheric anomalous anticyclone (Fig. 2: −12 to 0 pentads), further deepens the thermocline and warms the mixed layer more by reducing entrainment. The emergence of the equatorial easterly wind anomaly (Fig.1: −12 to 0 pentads) further strengthens the warming of the southwest Indian Ocean by anomalous meridional Ekman heat transport (Fig.7, third column: −12 to 0 pentads). The damping cooling effect of the sea surface net heat flux anomaly over the southwest Indian Ocean is enhanced (Fig.7, fifth column: −12 to 0 pentads and Fig.8b). During the extinction stage (0 to +80 days), the negative sea surface net heat flux anomaly dominates cooling of the southwest Indian Ocean.

To summarize, the sea surface net heat flux anomaly and zonal advective heat transport anomaly over the southern Arabian Sea and Somalia coast, respectively, are important for mixed layer warming during the initial stage of IOD events (from −24 to −12 pentads). Subsequently, the vertical entrainment anomaly becomes the primary driver, and the sea surface net heat flux anomaly takes the role of damping cooling close to the IOD events (−9 to 0 pentads). Although there is a clear meridional advective heat transport anomaly, the vertical entrainment anomaly has the dominant effect over the southwest Indian Ocean. It should be also noted that the sea surface net heat flux anomaly plays a more important role in damping the warming of the southwest Indian Ocean than that of the south Arabian Sea.

5 SUMMARY

This study utilized multiple reanalysis datasets, regression analysis, EOF analysis, and a $2^1/_2$ layer dynamic upper-ocean model to study the mechanism of warming in the southern Arabian Sea and the southwest Indian Ocean during the development of IOD events. The results are shown as follows.

During the initial stage of IOD events (−24 to −12 pentads), a warm downwelling Rossby wave excited by the anomalous anticyclone over the west Indian Peninsula leads to increased heat content in the upper thermocline and deepening of the thermocline, and further contributes to mixed layer warming by reducing entrainment cooling. An anomalous anticyclone over the west Indian Peninsula weakens the wind over the south Arabian Sea and Somali coast, which leads to further decrease in sea surface heat loss and shallowing of the surface mixed layer, which in turn amplifies the contribution of the net heat flux anomaly to the mixed layer warming; it also contributes to increasing SST in the south Arabian Sea by inhibiting entrainment, and along the Somali coast by inhibiting upwelling and zonal advection. As the IOD develops further (−9 to 0 pentads), the warming of the south Arabian Sea is mainly caused by vertical entrainment associated with the warm Rossby waves and wind anomaly, while the sea surface net heat flux results mainly from the damping cooling.

Anomalies in the wind speed and net sea surface heat flux are not significant over the southwest Indian Ocean during the initial IOD stages (−24 to −12 pentads). Warm downwelling Rossby waves excited by an anomalous anticyclone over the southwest Indian Ocean play the same role in the mixed layer warming as in the south Arabian Sea. Then, closer to the IOD maximum (−9 to 0 pentads), the superposition of warm westward downwelling Rossby waves excited by anomalous anticyclones over the Southwest Indian Ocean and southeast Indian Ocean respectively results in significant warming in the southwest Indian Ocean by a reduction in entrainment heat loss. At this time, meridional heat transport via Ekman flow excited by the equatorial east wind also plays a role in the warming of the southwest Indian Ocean. Additionally, the sea surface net heat flux mainly contributes to damping the warming of the south Arabian Sea and the southwest Indian Ocean, but it is more important for the latter.

Considering that El Niño may have an important effect on IOD, we also composite SSTA and surface

momentum flux anomalies for Co-occurrence El Niño and IOD and Pure IOD (figure omitted). It shows that the warming in northwest Arabian Sea is more closely related to El Niño while it is likely the result of local air-sea interaction in the southeast Arabian Sea. This is a very interesting scientific topic to our further study.

All of the findings above indicate that the warming mechanism in the Arabian Sea is very different from that of the Southwest Indian Ocean. There are more complicated factors contributing to the warming of the Arabian Sea. However, this paper only used a simplified ocean model to explore these mechanisms, especially the oceanic dynamics progress, in the warming of west Indian Ocean. Thus, a coupled model is needed in further research on air-sea interaction mechanisms over the Arabian Sea and the relationship between the Arabian Sea warming and the El Niño during the IOD events.

REFERENCES:

[1] SAJI N H, GOSWAMI B N, VINAYACHANDRAN P N, et al. A dipole mode in the tropical Indian Ocean [J]. Nature, 1999, 401 (6751): 360-363.

[2] WEBSTER P J, MOORE A M, LOSCHNIGG J P, et al. Coupled ocean-atmosphere dynamics in the Indian Ocean during 1997-98 [J]. Nature, 1999, 401 (6751): 356-360.

[3] YAMAGATA T, BEHERA S K, RAO S A, et al. Comments on "Dipoles, temperature gradients, and tropical climate anomalies" [J]. Bull Amer Meteorol Soc, 2003, 84 (10): 1 418-1 422.

[4] LI Chong-yin, MU Ming-quan. The influence of the Indian Ocean dipole on atmospheric circulation and climate [J]. Adv Atmos Sci, 2001, 18 (5): 831-843.

[5] XIE S P, ANNAMALAI H, SCHOTT F A, et al. Structure and mechanisms of south indian ocean climate variability [J]. J Climate, 2002, 15 (8): 864-878.

[6] LI T, WANG B, CHANG C P, et al. A Theory for the Indian Ocean Dipole-Zonal Mode [J]. J Atmos Sci, 2003, 60 (17): 2 119-2 135.

[7] WANG B, WU R, LI T. Atmosphere-Warm Ocean Interaction and Its Impacts on Asian-Australian Monsoon Variation [J]. J Climate, 2003, 16 (8): 1 195-1 211.

[8] YUAN Yuan, ZHOU Wen, YANG Hui, et al. Warming in the Northwestern Indian Ocean Associated with the El Niño Event [J]. Adv Atmos Sci, 2008, 25 (2): 246-252.

[9] GUAN Z, YAMAGATA T. The unusual summer of 1994 in East Asia: IOD teleconnections [J]. Geophys Res Lett, 2003, 30 (10): 235-250.

[10] YANG Ming-zhu, DING Yi-hui. Diagnostic study of the variation of Indian Ocean sea surface temperature and its impact on Indian summer monsoon rainfalls [J]. Acta Oceanol Sinica, 2006,28(4): 9-16 (in Chinese).

[11] YU Bo, GUAN Zhao-yong. Simulated structural changes of Asian summer monsoon circulation in association with indian ocean dipole sstas [J]. Trans Atmos Sci, 2009, 32 (6): 765-775 (in Chinese).

[12] GILL A E. Some simple solutions for heat-induced tropical circulation [J]. Quart J Roy Meteorol Soc, 1980, 106 (449): 447-462.

[13] TAN Yan-ke, LIU Hui-rong, LI Chong-yin. Possible causes for seasonal phase locking of the tropical Indian Ocean dipole [J]. Chin J Atmos Sci, 2008, 32(2): 197-205 (in Chinese).

[14] VINAYACHANDRAN P N, SAJI N H, YAMAGATA T. The response of the equatorial Indian Ocean to an unusual wind event during 1994 [J]. Geophys Res Lett, 1999, 26 (11): 1 613-1 616.

[15] MURTUGUDDE R, MCCREARY J P, BUSALACCHI A J. Oceanic processes associated with anomalous events in the Indian Ocean with relevance to 1997-1998 [J]. J Geophys Res, 2000, 105 (C2): 3 295-3 306.

[16] RAO S A, BEHERA S K, MASUMOTO Y, et al. Interannual subsurface variability in the tropical Indian Ocean with a special emphasis on the Indian Ocean dipole [J]. Deep Sea Res Part II: Topical Studies Oceanogr, 2002, 49(7): 1 549-1 572.

[17] YUAN D L, LIU H. Long-wave dynamics of sea level variations during Indian Ocean Dipole events [J]. J Phys Oceanogr, 2009, 39 (5): 1 115-1 132.

[18] WU R, KIRTMAN B P, KRISHNAMURTHY V. An asymmetric mode of tropical Indian Ocean rainfall variability in boreal spring [J]. J Geophys Res, 2008, 113 (D5): 79-88.

[19] DU Y, XIE S P, HUANG G, et al. Role of air-sea interaction in the long persistence of El Niño-induced North Indian Ocean warming [J]. J Climate, 2009, 22 (8): 2 023-2 038.

[20] GUO F Y, LIU Q Y, SUN S W, et al. Three types of Indian Ocean dipoles [J]. J Climate, 2015, 28 (8): 3 073-3 092.

[21] PRASAD T G, MCCLEAN J L. Mechanisms for anomalous warming in the western Indian Ocean during dipole mode events [J]. J Geophys Res Oceans, 2004, 109(C2): 235-250.

[22] GUO Fei-yan, LIU Qin-yu, ZEHNG Xiao-tong, et al. The role of barrier layer in southeastern Arabian Sea during the development of positive Indian Ocean dipole events [J]. J Ocean Univ China, 2013, 12 (2): 245-252.

[23] WILSON E A, GORDON A L, KIM D. Observations of the Madden Julian Oscillation during Indian Ocean Dipole events [J]. J Geophys Res: Atmos, 2013, 118(6): 2 588-2 599.

[24] RAO S A, LUO J J, BEHERA S K, et al. Generation and termination of Indian Ocean dipole events in 2003, 2006 and 2007 [J]. Clim Dyn, 2009, 33(6): 51-767.

[25] DU Y, LIU K, ZHUANG W. The Kelvin wave processes in the equatorial Indian ocean during the 2006-2008 IOD events [J]. Atmos Oceanic Sci Lett, 2012, 5: 324-328.

[26] MCCREARY J P, KUNDU P K. A numerical investigation of sea surface temperature variability in the Arabian Sea [J]. J Geophys Res: Oceans (1978-2012), 1989, 94 (C11): 16 097-16 114.

[27] MCCREARY J P, KUNDU P K, MOLINARI R L. A numerical investigation of dynamics, thermodynamics and mixed-layer processes in the Indian Ocean [J]. Prog O-

ceanogr, 1993, 31(3): 181-244.
[28] KRAUS E B, TURNER J S. A one dimensional model of the seasonal thermocline. II. The general theory and its consequences [J]. Tellus, 1967, 19(1): 98-106.

Citation: GUI Fa-yin, LI Chong-yin, TAN Yan-ke et al. The warming mechanism in the southern Arabian Sea during the development of Indian Ocean dipole events [J]. J Trop Meteorol, 2016, 22(2): 159-171.